Copyright 2022 Society of Photo-Optical Instrumentation Engineers. One print or electronic copy may be made for personal use only. Systematic reproduction and distribution, duplication of any material in this paper for a fee or for commercial purposes, or modification of the content of the paper are prohibited.
Joern-Holger Franke, Timothy A. Brunner, Eric Hendrickx, "Dual monopole exposure strategy to improve extreme ultraviolet imaging," J. Micro/Nanopattern. Mats. Metro. 21(3) 030501 (20 July 2022) https://doi.org/10.1117/1.JMM.21.3.030501

LETTER

Dual monopole exposure strategy to improve extreme ultraviolet imaging

Joern-Holger Franke,[a,*] Timothy A. Brunner,[b] and Eric Hendrickx[a]
[a]IMEC, Leuven, Belgium
[b]ASML Technology Development Center, United States

Abstract

Background: In extreme ultraviolet lithography, the printable feature density is limited by stochastic defectivity, which can be reduced by increasing the optical contrast. The photomask induces pole-specific aerial image offsets. Consequently, illumination settings with multiple poles lead to contrast loss and focus offsets between different features.

Aim: We aim to mitigate the contrast loss and best focus offsets between different features.

Approach: Illumination was decomposed into monopoles. Each monopole was exposed separately using a fraction of the total dose. Each exposure was shifted by its pole-specific image offset to mitigate 3D mask effects.

Results: Single monopoles mitigate contrast loss and best focus shifts, but in defocus, they suffer from aerial image shifts and distortions. Multiple aligned monopole exposures conserve these advantages but mitigate the problems in defocus. Because each monopole is exposed with only a fraction of the dose, the throughput penalty is limited to the scanner overhead.

Conclusions: A multiple monopole exposure scheme can increase contrast, align the best foci, and mitigate single monopole exposure constraints. Additionally, it offers an improved pattern placement control through dose control knobs.

© *2022 Society of Photo-Optical Instrumentation Engineers (SPIE)* [DOI: 10.1117/1.JMM.21.3.030501]

Keywords: extreme ultraviolet lithography; imaging; defectivity; monopoles; source optimization; vote taking.

Paper 22016L received Apr. 25, 2022; accepted for publication Jul. 1, 2022; published online Jul. 20, 2022.

1 Introduction

In recent years, extreme ultraviolet (EUV) lithography has enabled the continued downscaling of semiconductor devices.[1] The short wavelength of 13.5 nm enables the imaging of much denser features than is possible in deep ultraviolet lithography. However, EUV imagery brings with it specific challenges: all materials are strongly absorbing and have refractive indices close to unity at the 13.5-nm wavelength. As a result, light diffraction off this photomask is a highly complex problem.[2–5]

Somewhat surprisingly, it turns out that the most important consequence of the light being scattered off a complex 3D photomask is an image shift that depends on which diffraction orders are captured.[6] This shift is a consequence of the phase differences between diffraction orders.[7] In practice, EUV lithography uses off-axis illumination with sources that consist of multiple, usually opposing, poles. For each pole, different diffraction orders are captured, and the image shift is therefore be different. Opposing poles typically show pattern shifts of opposite signs. Importantly, this shift depends only weakly on the imaged pitch.

Superimposing images that are shifted against one another has important imaging consequences. First, we degrade image quality (i.e., we lose contrast).[7,8] This is especially problematic

*Address all correspondence to Joern-Holger Franke, joern-holger.franke@imec.be

1932-5150/2022/$28.00 © 2022 SPIE

in EUV lithography as high contrast is needed to reduce stochastic defectivity. Contrast variations will therefore translate into yield loss. It can potentially be countered by slowing down the resist to reduce the photon shot noise. This however translates to loss of throughput, with tangible economic consequences.

Another imaging consequence of the pole-specific pattern shifts is best focus offsets for different pitches. The range of best focus values observed through pitch is directly proportional to the pattern shift between the poles. Reducing the focus variation with pitch can improve the overlapped depth-of-focus (DOF) for printing logic metal patterns with multiple pitches in a single EUV exposure.[7]

One straightforward way to solve the abovementioned problems is to divide the exposure with the dipole illumination source into two monopole exposure passes with a relative image shift that corrects the pole-to-pole shift, a method that we call dual monopole exposure. In this paper, we show how the compensation of the pole-to-pole shift leads to increased contrast and mitigates best focus shifts. The improved contrast can also be accomplished with a single monopole exposure; however, overlay control through focus is severely compromised by the highly asymmetric source.[9,10] The opposing monopole in the dual monopole method re-establishes source symmetry, thus restoring overlay control in defocus.

The two passes of the dual monopole are more complicated than a normal single exposure, but they are not twice as slow because each monopole exposure pass uses half of the normal dose. The throughput of the dual monopole has some practical limitations, which will be discussed in a later section, and may preclude high volume manufacturing (HVM) applications at the present time.

This paper is structured as follows. In Sec. 2, we show how pole-to-pole offsets degrade imaging with dipole sources. In Sec. 3, we show how a dual monopole exposure scheme alleviates this problem. In Sec. 4, we discuss the practical advantages and shortcomings of the dual monopole exposure scheme. Finally, we summarize the conclusions in Sec. 5.

2 Dipole Exposure

We consider imaging a pitch $P = 32$-nm grating using an un-polarized EUV system with NA = 0.33, as in the NXE3400. Because this pitch is $< \lambda/\mathrm{NA}$, only two diffracted orders are involved in image formation, as schematically shown in Fig. 1. A single plane wave is incident on the mask, labeled the zeroth order in Fig. 1(a), at the telecentric position where $\sigma_0 = \lambda/(2\,\mathrm{NA}\,\mathrm{P})$. The grating on the mask diffracts a first-order beam to a pupil position equal but opposite to the zeroth-order beam, and these two beams then interfere to form a sinusoidal image at the wafer. The symmetry of the zeroth and first order with respect to the optical axis means that the image does not shift in the image plane when changing focus. This is why we call σ_0 "telecentric" sigma and the corresponding pitch telecentric pitch.[6] For a grating of vertically oriented lines at pitch 32 nm (P32V), there are two such telecentric source points, shown in Fig. 1(b) as an

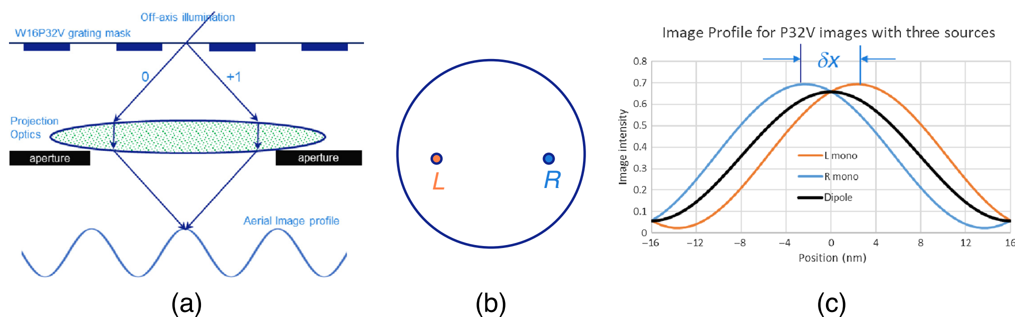

Fig. 1 (a) Projection imaging schematic for P32V imaging with monopole source at ideal telecentric point. (b) Pupil diagram of point dipole source optimized for P32V, indicating the *L* and the *R* monopoles. (c) Image profiles at best focus of the *L* monopole and *R* monopole showing the δx shift caused by phase effects. The point dipole image, in black, has reduced contrast from image fading.

Downloaded From: https://www.spiedigitallibrary.org/journals/Journal-of-Micro/Nanopatterning,-Materials,-and-Metrology on 25 May 2023
Terms of Use: https://www.spiedigitallibrary.org/terms-of-use

L monopole on the left and an R monopole on the right. Image profiles were calculated using a simulation program that takes full account of the 3D mask details, assuming a standard EUV mask with an Mo/Si multi-layer reflector, Ru capping layer, and 70-nm thick Ta absorber pattern.

Figure 1(c) shows the simulated image profiles of the L monopole in orange and the R monopole in blue. A key metric used to assess image quality is the image contrast C, defined as

$$C \equiv \frac{I_{\max} - I_{\min}}{I_{\max} + I_{\min}}, \tag{1}$$

where $I_{\max}$ and $I_{\min}$ are the extremes of the intensity profile. Both monopole images have high contrast, $C \approx 93\%$. Note the relative shift between the two monopole images, $\delta x \approx 4.6$ nm, a consequence of the phase difference between the zeroth- and first-order waves calculated by the detailed mask diffraction.

Even though the monopole images have high contrast, they are not normally used for chip production because of their extremely asymmetric, non-telecentric imagery for structures other than the one telecentric pitch, causing uncontrollable overlay errors with focus.[9,10] A normal dipole source shape would place two monopoles across from each other to achieve a symmetric source, e.g., Fig. 1(b). The net dipole image is the sum of the two monopole sub-images, and the δx relative shift causes a "fading" loss of contrast given by the factor[5]

$$C_{\text{fade}} = \cos\left(\frac{\pi \delta x}{P}\right). \tag{2}$$

The dipole image profile, shown in black in Fig. 1(c), has image contrast reduced to 82% due to this fading. For this P32 example with $\delta x = 4.6$ nm, $C_{\text{fade}} \approx 0.9$, i.e., a 10% contrast loss. δx varies by an insignificant 0.2 nm through the slit. The P in the denominator of Eq. (2) suggests that the smaller pitches of high-NA images may have even larger contrast losses from fading.

Another important imaging consequence of the δx pole-to-pole shift is pitch-dependent focus offsets. We demonstrate this using the P32V telecentric dipole source shown in Fig. 1(b). Image profiles for both the L and the R monopoles are calculated through focus for three different pitches: 28, 32, and 36 nm. Figure 2(a) shows the image shift variation with focus for these gratings, with solid points calculated for the R monopole and hollow points calculated for the L monopole. For the telecentric 32-nm pitch, the focus dependence is flat, and we see a constant 4.6-nm relative shift between the two images. Because the other two pitches are not telecentric, they shift linearly with focus because the image does not propagate parallel to the optical axis. Because the L pole shift and the R pole shift are not parallel, there will be a particular focus offset

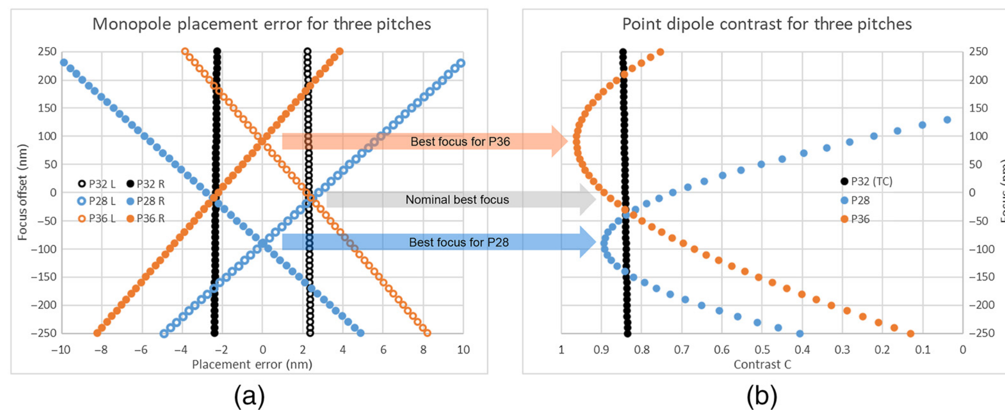

Fig. 2 (a) Image placement error plotted versus focus, for three different pitches. The L or R monopole source shown in Fig. 1(b) is assumed. (b) Image contrast versus focus, for P28V, P32V, and P36V resulting from the same dipole source. It is worth noting that maximum contrast occurs at the focus where the L and R images have zero relative shift. For all plots, the focus changes in the vertical direction.

Downloaded From: https://www.spiedigitallibrary.org/journals/Journal-of-Micro/Nanopatterning,-Materials,-and-Metrology on 25 May 2023
Terms of Use: https://www.spiedigitallibrary.org/terms-of-use

where the two lines cross, thus eliminating the fading loss of contrast. For the P28 images (in blue), the crossing point is at an approximate focus offset of −100 nm, whereas the P36 images (in orange) cross at a focus offset of +90 nm. At these special focus offsets, the fading is eliminated and image contrast is maximized, as shown in Fig. 2(b). The non-telecentric shift serves to cancel out the pole-to-pole shift and thereby achieve a higher contrast than the P32 telecentric image, at the cost of a pitch-dependent focus offset.[7,8]

We also note in Fig. 2(a) that the pole-to-pole shift calculated for all three pitches at the nominal best focus are virtually identical. This is not an assumption but a detailed result of the 3D mask diffraction calculation. If the mask had $\delta x = 0$ nm for all of the pitches, then the crossing point of the L and R sub-images would be at the nominal focus, and the most important mechanism for pitch-dependent focus offset would be eliminated. Also note that, for both pitch 28 nm and pitch 36 nm, only the first-diffraction order is captured. The pole-specific aerial image shifts are similar to this simple case for more relaxed pitches and even for 2D features.[7]

3 Dual Monopole Exposure

The Dual Monopole exposure method works as follows:

1. Expose a first pass with the first monopole using a fraction of the normal dose. For vertical lines and spaces (L/S), the dose is half of the total dose, whereas for horizontal L/S, it can vary.
2. Expose a second pass that is shifted to cancel out the pole-to-pole shift, i.e., to place the second monopole sub-image on top of the first pass, again using half of the normal dose. The shift compensation can be dialed in with sub-nm accuracy in modern EUV scanners.[11]

If these two passes are executed with zero shift between the passes, it is equivalent to a normal dipole exposure. But by correcting the δx pole-to-pole shift, the loss of contrast from fading, along with the focus offset, is eliminated.

Dipole and dual monopole image contrast C versus focus offset simulation results are shown in Fig. 3. First, we use the P32V telecentric point sources to obtain the results shown in Fig. 3(a). The normal dipole exposure results are shown as individual data points for P32, P28, and P36, identical to the curves from Fig. 2(b). The dual monopole results, using a 4.6-nm shift between exposures to cancel out δx, are shown as solid lines for the same three pitches. For the telecentric P32 exposures, shown in black, the dual monopole substantially boosts the best image contrast from 82% to 93% by eliminating the fading. The dual monopole exposure for the non-telecentric

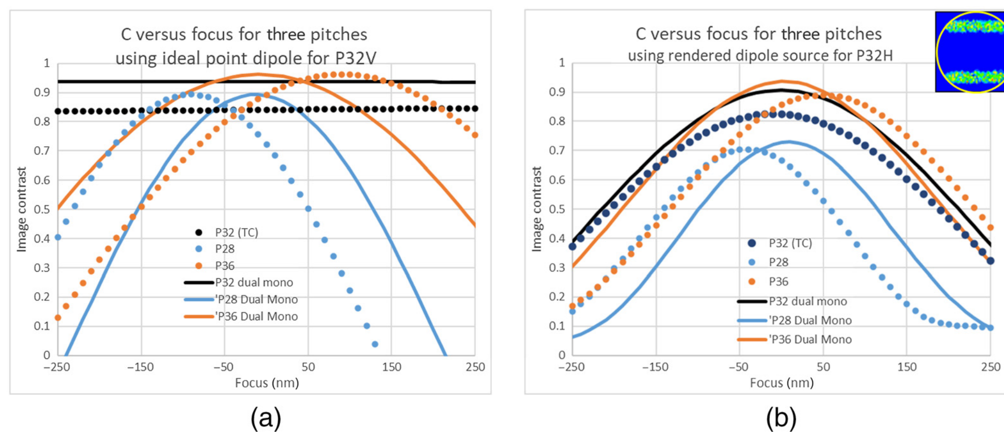

Fig. 3 (a) Image contrast C versus focus comparing dipole and dual monopole imaging for vertical L/S gratings with three different pitches, assuming the point dipole source from Fig. 1(b). P32 (TC) denotes that this pitch is where the source position was chosen to be telecentric. (b) Similar plots of C versus focus for horizontal L/S gratings. The upper right inset shows the source diagram, where the yellow circle shows the 0.33-NA pupil. The dual monopole images have higher contrast and smaller best focus offsets. In this example, the doses used for the two monopoles are identical.

Downloaded From: https://www.spiedigitallibrary.org/journals/Journal-of-Micro/Nanopatterning,-Materials,-and-Metrology on 25 May 2023
Terms of Use: https://www.spiedigitallibrary.org/terms-of-use

P28 and P36 shows best focus very close to nominal, unlike the dipole case. The elimination of best focus offsets for different pitches could be a significant advantage for achieving an improved common overlapped DOF for all structures.

So far, our simplified discussion assumed point sources, which are attractive theoretically but not practical. For our next calculations, we assume an extended and fully rendered dipole source that can be experimentally realized. Also, for simplicity, the initial discussion assumed vertical gratings where the left/right poles were perpendicular to the chief ray offset angle. We now rotate the grating lines to the horizontal orientation (P32H). The dipole source for P32H is no longer symmetric,[6] with one pole having a greater incidence angle onto the mask and a greater loss of intensity from shadowing. This is due to the chief ray angle of incidence being tilted by 6 deg toward the y axis in current EUV scanners using 0.33 NA. Figure 3(b) shows image contrast versus focus offset for horizontal gratings of three different pitches, using the P32H rendered dipole source shown. Once again, the individual data points show normal dipole results, and solid lines show dual monopole results. Compared with the point dipole sources [Fig. 3(a)], the rendered dipole focus offsets are somewhat smaller but still significant, in the ± 50-nm range. We also note that even the telecentric P32H images change contrast with focus because the rendered dipole has source points with $|\sigma_y|$ in the range from 0.5 to 0.8, which is only roughly centered on the ideal $\sigma_0 = 0.64$ telecentric position. Detailed image simulations show a relative image shift of $\delta y = 6.4$ nm between the images of the upper and lower poles, so this shift was used in the dual monopole contrast calculations shown as solid lines in Fig. 3(b). For P32H, there is roughly a 10% advantage over dipole, quite similar to that seen for the simplified P32V calculations with point dipoles.

The dual monopole exposures of P28H and P36H gratings now have best focus near nominal, greatly reducing the focus offsets seen for dipole. There is also a small improvement in the maximum contrast relative to dipole. Note that the lower contrast for P32H against P32V is due to the horizontal orientation of the L/S for which the optimum mask bias of each pole is different.

4 Practical Considerations

A feasibility study of dual monopole exposures is being conducted on the ASML NXE:3400B at imec. Initial data do not show fundamental issues. A more detailed report will be provided in a later publication. Historically, monopole exposures were hindered by an inability to align the reticle due to the highly non-telecentric images of the reticle alignment marks. The preferred solution to this problem is to perform the reticle alignment step using a more normal symmetric source shape and then to switch the source shape to the desired monopole for exposure.

We need sub-nm overlay between the images of the two exposure passes, which can be enabled by the wafer not leaving the chuck between the two exposures. Such a tight overlay between exposure passes has been demonstrated previously in the context of vote-taking,[12] in which the mask changes for each pass. For dual monopole, the mask could stay in place and only the source switches between passes, with a small stage offset used to compensate for the pole-to-pole image shift. More frequent source switching than normal may lead to throughput issues and illuminator lifetime issues. These issues can be partly mitigated by optimizing the exposure pass sequence: first expose wafer 1 with source 1 and then switch to source 2. Expose wafer 2 first with source 2 and then with source 1.

Another illuminator issue for dense metal layers is the small pupil fill ratio (PFR), for a monopole source nominally has half of the PFR of a dipole source. For the rendered dipole source shown in Fig. 3(b), PFR $\approx$22%, meaning that each of the two monopoles has PFR $\approx$11%. This has important throughput implications because, for current illuminators, PFRs <20% will reduce the illumination efficiency[13] and, thereby, directly reduce throughput. A mitigating factor on this problem is that dual monopole may be able to use fuller poles (with greater PFR) than the typical outer half or inner half leaf-shapes typically used today.

Another throughput detractor is the need to expose two separate passes. If the scan speed is "stage-limited," then the two scans would reduce throughput by half. More likely, the scan speed is "dose-limited" such that the two "half-dose" scans would be roughly twice as fast, and the

Downloaded From: https://www.spiedigitallibrary.org/journals/Journal-of-Micro/Nanopatterning,-Materials,-and-Metrology on 25 May 2023
Terms of Use: https://www.spiedigitallibrary.org/terms-of-use

throughput might only be reduced by 20%. These throughput considerations, along with the need to frequently change the source shape per wafer, may preclude HVM applications of dual monopole with current EUV expose tools.[13]

The expected dual monopole overlay performance is similar to a dipole. Perhaps a small improvement can be expected from the higher image contrast. Also, we can control pole balancing accurately via dose control, potentially providing another knob to control overlay through focus. However, care should be taken to balance imaging and overlay (through focus).

A dual monopole also makes the choice of source points per pole more flexible than what is possible for a single monopole. For a single monopole, we need to make the source telecentric for the basic pitch to keep non-telecentricities under control. With dual monopoles, this constraint is gone, and we can optimize the source point positions to optimize the printability of critical features such as non-dense L/S and tip-to-tip.

5 Conclusions

A dual monopole exposure scheme is discussed to improve the imaging in EUV lithography. The idea is to expose each pole of a dipole source separately at about half of the dose, with a shift between the two exposures to cancel the 3D mask-induced image offset. This removes the contrast loss from fading and mitigates pitch-dependent best focus shifts, as shown in the simulations.

There are different ways to mitigate pole-to-pole offsets[10] (aberration injection, single monopoles, and modified mask stacks). The dual monopole can be considered to be a fourth alternative that

1. Offers a more complete pole-to-pole offset correction than aberration injection.[7]
2. Does not suffer from uncorrectable image displacement in defocus as single monopoles do.[10]
3. Does not require a new mask stack.[3–5]
4. Is potentially more extendable toward contact hole patterns than aberration injection using, e.g., two opposing poles of a quadrupole illumination as monopoles.

Dual monopoles effectively provide a way to image standard Ta-based absorber masks without the offsets between images from opposing poles. Thus, all advantages coming from the symmetry of the dipole aerial image are conserved.

At the present time, dual monopole exposure may not be suitable for HVM, mainly due to throughput limitations. EUV illuminator developments are needed to support full illumination efficiency at reduced pupil fill ratio. Also, the scanner overhead incurred for exposing a wafer in two exposure passes at around half of the dose versus one exposure pass at full dose must be kept low. Although throughput blocks full production applications, dual monopole exposures could immediately be used for research or low volume applications in which throughput is not a dominant consideration. Potentially, it could be useful for boosting yield on a critical layer holding up overall yield for which throughput hits could be acceptable.

References

1. E. Verhoeven et al., "0.33 NA EUV systems for high volume manufacturing," *Proc. SPIE* **11517**, 1151703 (2020).
2. A. Erdmann et al., "Characterization and mitigation of 3D mask effects in extreme ultraviolet lithography," *Adv. Opt. Technol.* **6**(3–4), 187–201 (2017).
3. A. Erdmann et al., "Perspectives and trade-offs of absorber materials for high NA EUV lithography," *JMMM* **19**(4), 041001 (2020).
4. C. van Lare et al, "Investigation into a prototype extreme ultraviolet low-n attenuated phase-shift mask," *JMMM* **20**(2), 021006 (2021).
5. M. Burkhardt, "Investigation of alternate mask absorbers in EUV lithography," *Proc. SPIE* **10143**, 1014312 (2017).

Downloaded From: https://www.spiedigitallibrary.org/journals/Journal-of-Micro/Nanopatterning,-Materials,-and-Metrology on 25 May 2023
Terms of Use: https://www.spiedigitallibrary.org/terms-of-use

6. C. T. Shih et al., “Mitigation of image contrast loss due to mask-side non-telecentricity in an EUV scanner,” *Proc SPIE* **9422**, 94220Y (2015).
7. J.-H. Franke et al., “Improving exposure latitudes and aligning best focus through pitch by curing M3D phase effects with controlled aberrations,” *Proc. SPIE* **11147**, 111470E (2019).
8. M. Burkhardt et al., “Investigation of mask absorber induced image shift in EUV lithography,” *Proc. SPIE* **10957**, 1095710 (2019).
9. J.-H. Franke et al., “Metal layer single EUV expose at pitch 28 nm: how bright field and NTD resist advantages align,” *Proc. SPIE* **11609**, 116090R (2021).
10. D. Rio et al, “Extending 0.33NA EUVL to 28 nm pitch using alternative mask and controlled aberrations,” *Proc. SPIE* **11609**, 116090T (2021).
11. J.-H. Franke, E. H. Hendrickx, and G. C. Schiffelers, “Method and apparatus for photolithographic imaging,” European Patent Application WO 2020/221556A1 (2020).
12. J. Bekaert et al., “EUV vote-taking lithography: crazy... or not?” *Proc. SPIE* **10583**, 105830I (2018).
13. M. van de Kerkhof et al., “Enabling sub-10 nm node lithography: presenting the NXE: 3400B EUV scanner,” *Proc. SPIE* **10143**, 101430D (2017).

Downloaded From: https://www.spiedigitallibrary.org/journals/Journal-of-Micro/Nanopatterning,-Materials,-and-Metrology on 25 May 2023
Terms of Use: https://www.spiedigitallibrary.org/terms-of-use